Modelling of Profile Control with LH Wave Injection in the HL-2A Single-null Divertor Plasma[1]

Qingdi Gao 1), Baoshan Yuan 1), R. V. Budny 2), Fangzhu Li 1), Aike Wang 1)

1) Southwestern Institute of Physics, Chengdu, Sichuan, P. R. China
2) Princeton Plasma Physics Laboratory, Princeton University, Princeton, NJ, USA

e-mail contact of main author: qgao@swip.ac.cn

Abstract. In the HL-2A tokamak a single-null divertor configuration has been established. The separatrix of the single-null diverted plasma was identified with a filament model, and the determined striking area on the target plate is in agreement with the measurements of electric probe array. Higher power LH wave (1.5MW) is injected to the diverted plasma with a nearly symmetric spectrum. Dominant electron heating and current profile control are investigated with numerical simulation. Plasma heating by electron Landau interaction results in operation scenarios of preferentially dominant electron heating. Due to the off-axis driven current, an optimized q-profile is formed, and an enhanced confinement regime with steep electron temperature gradient is produced. The clear decrease of the electron thermal conductivity in the LH power deposition region shows that an electron-ITB is developed. When higher LH power injects into the target plasma that is heated by NBI (0.5MW), the ion temperature has a large increment in addition to the high increase of electron temperature. The temperature profiles indicate that an enhanced core confinement is established with both ion-ITB and electron-ITB developed.

1. Introduction

In the HL-2A tokamak, a single-null divertor (SND) configuration has been established in recent Ohmic discharges. In order to raise the plasma parameters and achieve more interesting operation scenarios in HL-2A [1] as early as possible, a campaign to carry out plasma heating using the available auxiliary heating schemes is essential. Now the auxiliary heating scheme of lower hybrid wave (3 klystrons with power up to 2.0 MW at frequency f=2.45GHz) is available, and it had been successfully used in the HL-1M tokamak for current drive [2,3]. To know the prospective operation scenario upon injection of higher power LH wave into the single-null divertor plasma, the effectiveness of plasma heating by electron Landau interaction is investigated with numerical simulation.

Significant progress has been achieved in reducing anomalous energy transport in tokamak plasmas. In addition to the well-known improved H-mode regime with a transport barrier at the plasma edge, recent experiments performed in most tokamaks have shown that spontaneous reduction in anomalous transport can also occur inside the plasma core to form an internal transport barrier (ITB). Though the ion-ITB, which manifests itself by higher gradient of ion temperature inside it, has been studied extensively, the database and the physics understanding of electron-ITBs (eITB) are not so much extended as those of ion-ITB. In many tokamaks, such as RTP, FTU, DIII-D, TCV, ASDEX Upgrade, JT-60U and T10 [4-10], electron cyclotron resonance heating (ECRH) has been used to enter in improved confinement electron mode and eITBs have been observed. Most of the experiments were done in conditions of dominant electron heating in low collisional plasma. By using the available lower hybrid scheme in HL-2A, the plasma heating by electron Landau interaction can establish operation scenarios of preferentially dominant electron heating in low density plasmas.

---

[1] This work is supported by the National Natural Science Foundation of China under grant No. 10275018

The plasma transport through electron channel is larger than the neoclassical prediction by about two orders of magnitude, which is attributed to micro-turbulence. The electron transport is affected by turbulence of all wavelength, that is short wavelength ($k_\theta \rho_s > 1$, where k_θ is the poloidal wave vector and ρ_s the ion gyro-radius calculated at $T_e = T_i$) like electron temperature gradient mode (ETG), intermediate wavelength ($k_\theta \rho_s \sim 1$) like trapped electron mode (TEM), and long wavelength ($k_\theta \rho_s \sim 0.1$) turbulence like ion temperature gradient mode (ITG). Gyrofluid simulation [11] and gyrokinetic simulation [12] have found the stabilizing effect of negative shear and large pressure gradient in the ($\hat{s} - \alpha$) ballooning diagram (where $\hat{s}$ is the magnetic shear, $\alpha = -q^2 R\beta'$) on the TEM/ETG instabilities. Thus, control of the current profile is an important means to reduce anomalous transport in the electron channel. As the LH wave is of efficient current drive capability, it can be used to control the current profile to form reversed magnetic shear (RS) configuration in HL-2A.

2. Flux geometry of single-null divertor configuration

A fast algorithm is elaborated for identifying the plasma boundary from measurements performed with the pick-up coils and magnetic flux loops. The algorithm is based on modeling the plasma current by movable current filaments, and it aims at being applied to real-time data processing (on-line mode). The algorithm was tested in a series of model discharges under conditions typical of the HL-2A tokamak. By using the algorithm, separatrix of the SND plasma was identified, and the determined striking area on the target plate is in agreement with the measurements of electric probe array. As an example, the measured plasma boundary of shot 1776# at t = 0.23s is shown in Fig. 1.

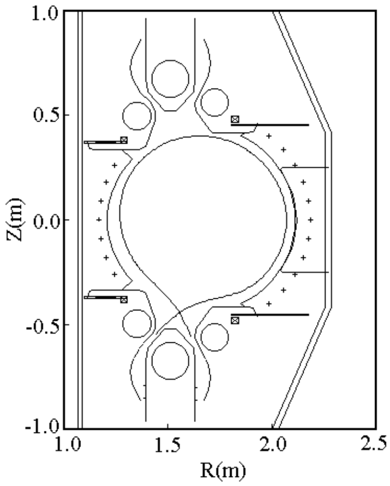

FIG.1. Plasma boundary of a single-null divertor discharge (shot 1766#) in HL-2A, identified by a filament model

In the simulated discharge, the plasma current ramps up to the maximum during ~ 0.3 second and then maintain a flat-top for about 1.6 second. The boundary (such as the 99.9% flux surface of the plasma) of the SND plasma that has been determined in the HL-2A discharge is used to describe the plasma geometry. The boundary is specified as a function of time, which evolves from a circular limiter plasma to a SND plasma as shown in Fig. 1 during the first 0.35s and then retains the same boundary in the flat-top phase. The interior flux surfaces are computed by solving the Grad- Shafranov equation. The flux geometry of the SND plasma is shown in Fig.2 where the boundary surface is designated $\rho = 1$, where ρ is defined as the square-root of normalized toroidal flux. The boundary surface is up-down asymmetric with different triangularity shaping for up-half plasma and low-half plasma. The lower triangularity is $\delta_L = 0.25$, but the upper triangularity $\delta_U \sim 0$. Though the plasma has a mildly shaped boundary, the flux surfaces inside plasma are nearly circular.

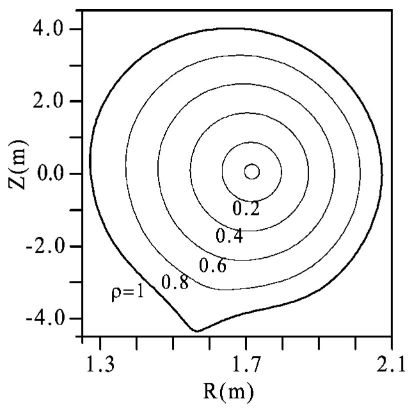

FIG. 2. Magnetic flux surfaces computed by solving the Grad -Shafranov equation with the boundary (99.9% flux surface) as shown in FIG. 1 used.

3. LH wave absorption by Landau damping

By choosing a local Cartesian coordinate system [13], such that $\hat{z} \times \vec{B} = 0$ and $\vec{k}$ is contained in the x-z plane:

$$\vec{k} = k_{//}\hat{z} + k_{\perp}\hat{x}\,, \qquad (1)$$

the LH wave dispersion relation is decomposed into its real and imaginary parts,

$$D = D_r + iD_i = 0 \qquad (2)$$

with

$$D_r = -\alpha k_{\perp}^6 + \varepsilon_{\perp} k_{\perp}^4 + [(\varepsilon_{//} + \varepsilon_{\perp})(k_{//}^2 - \varepsilon_{\perp} k_0^2) + \varepsilon_{xy}^2 k_0^2] + \varepsilon_{//}[(k_{//}^2 - \varepsilon_{\perp} k_0^2)^2 - \varepsilon_{xy}^2 k_0^4] \qquad (3)$$

$$D_i = \frac{\partial D_r}{\partial \varepsilon_{//}} K_{zz,i} \qquad (4)$$

where $\vec{k}$ is the wave vector, $k_0 = \omega / c$, $\varepsilon_{//}$, $\varepsilon_{\perp}$, and ε_{xy} are components of the dielectric tensor for a cold plasma, α is the thermal term that would be important near lower hybrid resonance,

$$\alpha = \frac{3}{4}\frac{\omega_{pe}^2}{\omega_{ce}^4} v_{Te}^2 + 3\frac{\omega_{pi}^2 v_{Ti}^2}{\omega^4} \qquad (5)$$

where ω is the LH wave frequency, ω_{ce} is the electron gyro-frequency, ω_{pe} and ω_{pi} are the plasma frequencies, v_{Te} and v_{Ti} are the thermal velocities. The anti-Hermitian part of the dielectric tensor $\overleftrightarrow{K}$ is retained as a perturbation. Here, the principal such term enters as an imaginary correction to K_{zz}, which describes the Landau damping of the LH wave in plasmas, namely the interaction between the wave electric field component parallel to $\vec{B}$ and electrons whose speed along $\vec{B}$ matches that of the wave:

$$K_{zz,i} = -\pi \frac{\omega_{pe}^2}{\omega} \int dv_{//} v_{//} \frac{\partial f_e}{\partial v_{//}} \delta(\omega - k_{//} v_{//}) \qquad (6)$$

where $v_{//}$ is the electron velocity component parallel to the magnetic field, and $f_e(v_{//})$ is a parallel velocity distribution function of electrons normalized such that $\int dv_{//} f_e(v_{//}) = 1$.

The calculation for the LH wave absorption utilizes a toroidal ray-tracing algorithm for the wave propagation and a parallel velocity Fokker-Planck calculation for the interaction of waves and particles. A spectral component of power W experiences a change ΔW over time interval $\Delta\tau$:

$$\Delta W = -2D_i \Big/ \left(\frac{\partial D_r}{\partial \omega}\right) W \Delta r = -2 \frac{\partial D_r}{\partial \varepsilon_{//}} K_{zz,i} \Big/ \left(\frac{\partial D_r}{\partial \omega}\right) W \Delta r$$

$$= 2\pi \frac{\omega_{pe}^2}{\omega} \int dv_{//} v_{//} \delta(\omega - k_{//} v_{//}) \times \frac{\partial D_r}{\partial \varepsilon_{//}} \Big/ \left(\frac{\partial D_r}{\partial \omega}\right) W \Delta r \qquad (7)$$

The current driven on each flux surface is calculated according to

$$j_{LH} = \frac{-en_e}{\nu_r} \int dv_{//} D_{ql}(v_{//}) \frac{\partial f_e(v_{//})}{\partial v_{//}} \frac{\partial W_s(u)}{\partial u} \qquad (8)$$

where $\nu_r = (\ln\Lambda) n_e e^4 / 4\pi\varepsilon_0^2 m_e^2 |v_r|^3$, $u = v_{//} / v_r$

$$D_{ql}(v_{//}) = \frac{\pi}{2}\left(\frac{e}{m_e}\right)^2 E_{//}^2 \delta\left(\omega - k_{//} v_{//}\right), \qquad (9)$$

$$v_r = -\mathrm{sgn}(eE_{DC})\sqrt{n_e e^4 \ln\Lambda / 4\pi\varepsilon_0^2 m_e |eE_{Dc}|} \quad . \qquad (10)$$

The key quantity is $W_s(u)$, the energy (normalized to $m_e v_r^2/2$) imparted to the electric field E_{DC} by an electron as it slows down.

4. Lower hybrid wave heating and eITB

The LH wave is injected with a multi-junction launcher (2×12) in HL-2A. The radiated power spectrum by the launcher is calculated with the Brambilla coupling theory [14]. The calculated spectrums for different relative waveguide phasing ($\Delta\varphi$) are shown in Fig. 3. The asymmetric power spectrum ($\Delta\varphi$ = 90°) is used for current drive, and the symmetric spectrum ($\Delta\varphi$ = 180°) is used for plasma heating. In order to produce some non-inductive current to control the current profile, in the LH heating simulation a nearly symmetric spectrum of $\Delta\varphi$ = 170° is assumed. The Brambilla coupling calculation combined with the LH absorption calculation is in conjunction with the TRANSP code to obtain the plasma heating in a dynamic case. The local electric field E_{DC} is supplied by TRANSP as part for iteration.

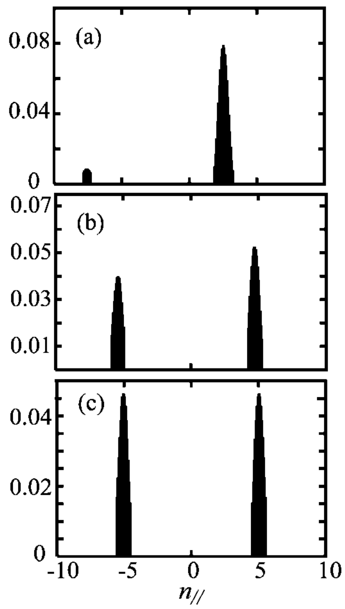

FIG. 3. Relative LH wave power versus $n_{//}$. (a) $\Delta\varphi$ = 90° (b) $\Delta\varphi$ = 170° (c) $\Delta\varphi$ = 180°

The energy transport model is a mixed theory model. Normally the transport observed in tokamak experiments greatly exceeds that of collisional transport theory. However, no theoretical model has yet been proposed which adequately describes all of the many features displayed by tokamak transport. Here, the ion heat diffusivity is assumed in terms of neoclassical transport enhanced by η_i turbulence. The electron energy transport is based on the Rebut-Lallia-Watkins (RLW) model [15] which, from heuristic and dimensional arguments, introduces a critical electron temperature gradient ∇T_{ec} such that the electron heat flow is neoclassical when $|\nabla T_e| < |\nabla T_{ec}|$ or $\nabla q < 0$. The distinctive feature of this hybrid model is that both η_i model and RLW model have been tested against a wide range tokamak devices [16].

Scenario of the low-density plasma heated by higher LH power is investigated. The parameters of the target plasma are: $I_p = 220kA$, $B_T = 2.0T$, and $\bar{n}_e = 1.0\times10^{19}m^{-3}$, deuterium gas. 1.5 MW LH wave power is injected during the flattop phase (t =0.7 – 1.2s). Due to higher power electron Landau heating, electron temperature increases significantly. The central electron temperature is about 0.6 *keV* before injection of the LH wave, and rises to more than 1.4 *keV* during the LH heating phase. In contrast to the large increment of the electron temperature, the ion temperature only has a small change (namely, the central T_i rise $\Delta T_{i0} \approx 0.17keV$ from the Ohmic value T_{i0} = 0.45 *keV*) because of low plasma density.

Since parallel refractive index of the used LH power spectrum ($\Delta\varphi$ = 170°) is rather high (the central refractive index $n_{//0} \approx 5.0$), the injected LH wave with lower phase velocity can be absorbed in outer region resulting in off-axis electron heating (Fig. 4a). The wave deposition region is also determined by analyzing the LH wave propagation domain in the (x,

$n_{//}$) phase space [17]. Constraint imposed by the wave propagation condition limits the maximum allowed $n_{//}$ upshift in the central plasma. Taking into account the Landau damping condition, it is concluded that LH power deposits off-axis. In addition to the plasma heating, a non-inductive current ($I_{LH} \approx 80kA$) is driven by the LH wave because of the slight asymmetry of the LH wave spectrum and the asymmetry of electron velocity distribution function caused by the electric field, E_{DC}. Due to the off-axis driven current, an optimized q-profile, of which the magnetic shear is weak in the central region and negative in the mid-plasma region ($x \approx 0.5 - 0.65$), is formed (Fig. 4c).

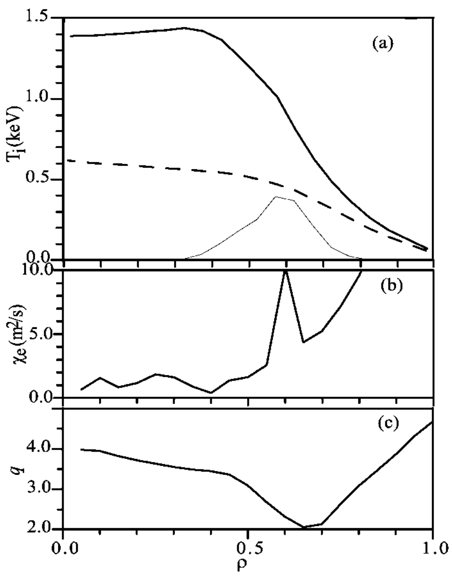

FIG. 4. (a) Electron temperature profiles during LHH (full line) and before LHH (dashed line). Fainter line indicates the location of LH absorption; (b) Electron thermal conductivity versus ρ*; (c) q-profile.*

The Ohmic and RF profiles of electron temperature are plotted in Fig. 4a. The RF profile corresponds to 200ms later after the RF has been turned on. LH heating raises electron temperature significantly and a steep temperature gradient is formed around the power deposition region. The normalized gradient R/L_T (where $L_T^{-1} = \nabla T_e / T_e$) at the steepest gradient, where ρ = 0.65, and the electron temperature T_e = 0.75*keV*, is R/L_T = 18, which exceeds largely the critical gradient value (R/L_T <10) for temperature profile stiffness [18]. The critical gradient is due to short or intermediate wavelength ETG/TEM instabilities. The large R/L_T value is consistent with the expected stabilizing effect of weak or negative shear on ETG/TEM instabilities. In FTU and DIII-D [5,6], ECRH has been used during fast current ramps to obtain negative or flat q profile by exploiting the skin effect. In the FTU experiment the eITB was developed with extremely high temperature gradient. The maximum normalized gradient of R/L_T = 19 was obtained, implying that the plasma behaves as it is far from the stiff critical gradient. In DIII-D, eITB was established with injecting ECRH off-axis into a low-density plasma, and an extreme steep temperature gradient was formed outside the power deposition region. The gyrokinetic linear stability analysis on DIII-D showed that the experimentally measured ∇T_e at the barrier was very close to the expected critical gradient for ETG mode, provided the stabilizing effect of negative shear and large pressure gradient in the ($\hat{s} - \alpha$) ballooning diagram was included in the calculation to reduce the turbulence growth rate.

As in the case of ion-ITB one would clarify an eITB when a clear decrease of the electron thermal conductivity is observed at the steep temperature gradient or in the region inside it. The simulation results show that the electron thermal conductivity is reduced obviously at the steep temperature gradient and in the central plasma region (Fig. 4b).

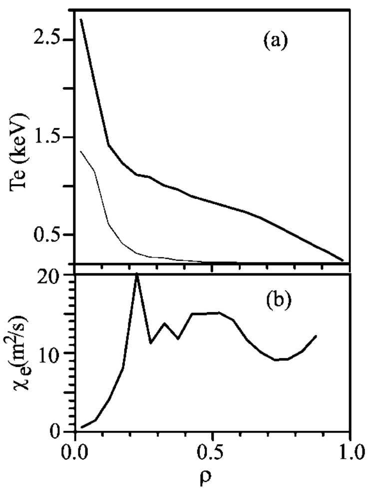

FIG. 5. (a) Electron temperature profile. Fainter line indicates the location of LH absorption; (b) Electron thermal conductivity versus ρ.

Since the electron temperature is still quite low at the start time of LH heating, LH waves can be deposited in the plasma center during a very short period after the LH wave injection. The central deposition of LH waves produces high central electron temperature (T_{e0} > 2.7*keV*), forming a narrow core region with very steep electron temperature gradient (Fig. 5a). Corresponding to the high central electron temperature, the electron thermal diffusivity in the plasma center is reduced significantly (Fig. 5b), which indicates an eITB is established in the central plasma region. However, this central improved confinement regime is transient.

To realize plasma heating and current profile control by using LH wave, an alternative way is that the LH wave is injected by two antennae: one is used to radiate symmetric spectrum ($\Delta\varphi$ = 180°) for heating, and one radiates asymmetric spectrum ($\Delta\varphi$ = 90°) for current drive. By adjusting the LH power for current drive, a discharge with similar characteristics as in the one-antenna case could be obtained. With 1.5MW LH power used for heating and 0.13MW for LHCD, the electron temperature profile and *q* profile similar to the profiles shown in Fig. 4 were produced.

5. Enhanced ion confinement

An NBI line with lower beam energy (E_b = 20-25*keV*) has been used for perpendicular injection in the HL-1M tokamak [19,20]. Now it can be used to heat the low-density plasma in HL-2A. The low-density plasma as described above is heated by co-injected NBI (P_{NB} = 0.5*MW*) during 0.5-1.8s, and then a higher LH power (P_{LH} = 1.5*MW*) is injected during 1.0 -1.5s, with the same launched spectrum as in the above case, to heat the plasma further and keep the q-profile reversed. During the LH wave injection phase, not only the electron temperature has a large increment, but the ion temperature increases significantly (from T_{i0} = 1.5*keV* to $T_{i0} \geq$ 2.6*keV*) as well. The temperature profiles as shown in Fig. 6 indicate that an enhanced core confinement regime is established with both ion-ITB and eITB in the LH heating phase.

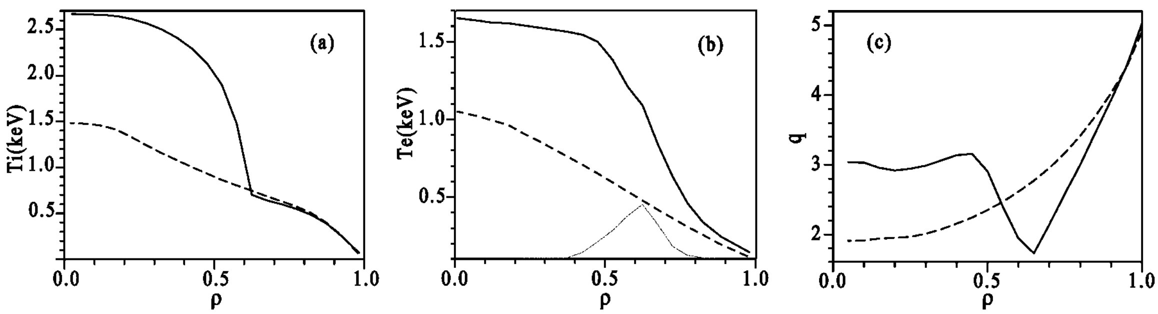

FIG. 6. (a) Ti – profile, (b) Te – profile (fainter line indicates the location of LH wave deposition), (c) q – profile. Dashed lines corresponding to the case of NBI heating only at t=0.9s, and full lines corresponding to the case of the NBI+LH heating at t=1.2s

Though the increase of T_e caused by the LH heating increases rate of the NBI energy loss to bulk ions, the fraction of NBI power that goes into the thermal ions (~ 0.21*MW*) is nearly unchanged in the LH injection phase since the NBI power loss due to charge-exchange and thermalization of the fast ions increases as well. For low density plasma the effect of electron -ion equipartition is negligible. Thus, compared to the case of NBI heating only, the large increment of T_i within the transport barrier is mainly attributed to the reduction of ion heat transport that is resulted from the magnetic shear optimization.

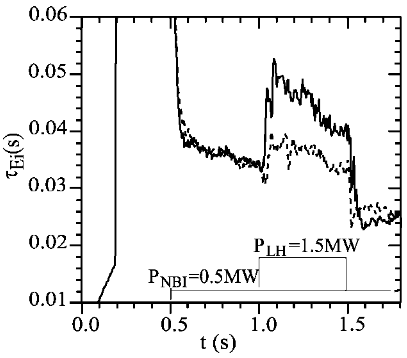

FIG. 7. Ion energy confinement time, τ_{Ei}, versus time for the simulated discharge with LH wave injected with slightly asymmetric spectrum (full line), and with purely symmetric spectrum (dotted line)

To illustrate the positive effects of the RS configuration on confinement in the ion channel, a comparison for the ion confinement is made between the RS and non-RS plasma. When the same power of LH wave is injected with purely symmetric spectrum ($\Delta\varphi$ = 180°) in the above discharge, the q-profile with reversed shear could not be formed since the off-axis current driven by the LH wave is not sufficient. In this case, only $T_{i0} \approx 2.0 keV$ is obtained, and the ion energy confinement time reduced by 20-25% with respect to the RS case (Fig. 7). Nevertheless, the ion energy confinement time is still higher than the pure NBI heating phase, which is consistent with the modification of the plasma current profile because the central magnetic shear is rather weak due to the non-inductive current that is resulted from the asymmetry of electron velocity distribution function caused by the electric field.

6. Summary

Lower hybrid wave is injected into a single-null divertor plasma in HL-2A. Dominant electron heating and current profile control are investigated with numerical simulation. The magnetic flux surfaces are calculated by solving the Grad-Shafranov equation by using the diverted plasma boundary that is determined from the HL-2A discharge. The LH wave power spectrum radiated by a multi-junction launcher (2×12) is calculated with the Brambilla's coupling theory. Analysis of the LH wave absorption utilizes a toroidal ray-tracing for the wave propagation and a parallel velocity Fokker-Planck calculation for the interaction of waves and particles. The LH absorption calculation combined with the Brambilla coupling calculation is in conjunction with the TRANSP code to obtain the plasma heating in a dynamic case.

Scenario of the low-density plasma heated by higher LH power is investigated. Plasma heating by electron Landau interaction results in operation scenarios of preferentially dominant electron heating. When LH wave (P_{LH} = 1.5MW) is injected to a low-density plasma with the relative wave-guide phase $\Delta\varphi$ = 170°, a non-inductive current ($I_{LH} \approx 80kA$) is driven in addition to the plasma heating. Due to the off-axis driven current, an optimized q-profile is formed, and enhanced confinement regime with steep electron temperature gradient is produced. The clear decrease of the electron thermal conductivity in the LH power deposition region shows that an eITB is developed. At the start time of the wave injection, LH power can be deposited in the plasma center to form a central improved confinement regime.

The simulation of LH heating in a target plasma that is heated by NBI (0.5 MW) shows that the modification of current profile caused by the LH driven current is favorable to enhancement of the ion energy confinement. As higher LH power injected into the NBI heated plasma with slightly asymmetric spectrum ($\Delta\varphi$ = 170°), which produces RS configuration, the ion temperature has a large increment in addition to the high increase of electron temperature. The temperature profiles indicate that an enhanced core confinement is established with both ion-ITB and electron-ITB developed. Nevertheless, when the same LH power is injected into the NBI heated plasma with purely symmetric spectrum ($\Delta\varphi$ = 180°), only much lower ion temperature can be obtained, and the ion energy confinement time is reduced by 20-25% with respect to the RS case.

References

[1] Gao, Q. D., et al., Nucl. Fusion **40 (**2000) 1897
[2] Liu, Y. et al., Fusion Energy 1998 (Proc. 17th Int. Conf. Yokohama, 1998), IAEA, Vienna (1999), CD-ROM file EXP2/17
[3] Ding, X. T., et al., in Controlled Fusion and Plasma Physics (Proc. 25th Eur. Conf. Prague, 1998), Vol. 22C, European Physical Society, Geneva (1998) 695
[4] Lopes Cardozo, N., et al., Plasma Phys. Control. Fusion **39** (1997) B303
[5] Buratti, P., et al., Phys. Rev. Lett. **82** (1999) 560
[6] Prater, R., et al., Fusion Energy 2000 (Proc. 18th Int. Conf. Sorrento, 2000), IAEA, Vienna (2001), CD-ROM file EX8/1
[7] Pietrzyk, Z. A., et al., Phys. Rev. Lett. **86** (1999) 1530
[8] Wolf, R. C., et al., Phys. Plasmas **7** (2000) 1839
[9] Ikeda, Y., at al., Fusion Energy 2000 (Proc. 18th Int. Conf. Sorrento, 2000), IAEA, Vienna (2001), CD-ROM file EXP4/03
[10] Razumova, K. A., et al., Plasma Phys. Report **27** (2001) 273
[11] Beer, M. A., et al., Phys. Plasmas **4** (1997) 1792
[12] Jenko, F., et al., Phys. Plasmas **7** (2000) 1904
[13] Stix, T. H., *Waves in Plasmas*, American Institute of Physics, New York (1992)
[14] Brambilla, M., Nucl. Fusion **16** (1976) 47
[15] Rebut, P. H., et al., Phys. Fluids **B3** (1991) 2209
[16] Conner, J. W., Plasma Phys. Control. Fusion **37** (1995) A119
[17] Gao, Q. D, et al., Nucl. Fusion **43** (2003) 982
[18] Ryter, F., et al., Plasma Phys. Control. Fusion **43** (2001) A323
[19] Yan, L. W., et al., Chin. Phys. Lett. **20** (2003) 1795
[20] Jiang, S. F., et al., in Controlled Fusion and Plasma Physics (Proc. 26th Eur. Conf. Maastricht, 1999), Vol. 23J, European Physical Society, Geneva (1999) 529